

# Defect Induced Thickness Growth in Silver Chloride (111) Tabular Crystals: A TEM Study.

W. Van Renterghem<sup>a</sup>, D. Schryvers<sup>a</sup>, J. Van Landuyt<sup>a</sup>, D. Bollen<sup>b</sup>, C. Van Roost<sup>b</sup> and R. De Keyzer<sup>b</sup>

<sup>a</sup> EMAT, University of Antwerp, Groenenborgerlaan 171, B-2020 Antwerpen

<sup>b</sup> Agfa-Gevaert N.V., Septestraat 27, B-2640 Mortsel

## Abstract

Defects in AgCl tabular crystals with {111} surfaces are characterised by transmission electron microscopy (TEM) and their influence on the growth process is discussed. In the tabular crystals, twins parallel to the tabular face as well as dislocations along different directions are observed. The twins induce the tabular growth, while the dislocations do not influence the morphology. In 10 to 30 % of the crystals that have been characterised, thickness growth is observed and it is shown that in all cases twins on other planes than the tabular ones are present. Two configurations occur more frequently and are analysed in detail. For the first group, twins parallel to the tabular face as well as a microtwin along a non-parallel {111} plane and ending inside the crystal are present. In the crystals of the second group only one extra non-parallel twin occurs giving rise to a bicrystal built up by a tetrahedral shaped part and a flat triangular or trapezoidal part. More complex twin configurations give rise to various, less characteristic morphologies.

## 1. Introduction

Populations of silver bromide crystals, produced at high bromine concentrations, mostly consist of tabular crystals<sup>1</sup>. Under these conditions, twins are easily formed and the {111} faces are the most stable crystal surfaces. In every tabular crystal, two or three twin planes parallel to the basal plane are present that induce tabular growth<sup>2</sup>. For AgBr, it is possible to produce populations that contain up to 97 % of tabular crystals.

Silver chloride has the advantage that it develops more rapidly and that it is more easily bleached and fixed. However, it is not possible to produce AgCl tabular crystals in the same way as for AgBr because, due to the high ionic charges, the {111} surfaces of a silver chloride crystal are not stable in an aqueous environment.

One solution to overcome this problem is the addition of a stabiliser for the {111} surfaces. Different stabilisers have been tested<sup>3,4</sup>, with adenine giving the best results and being commonly used. However, when precipitated under the same conditions as for AgBr, still 10 to 30 % of the AgCl crystals also grow in the third dimension, despite the addition of adenine. Due to the larger volume, these thick

crystals take up at least 30 % of the total amount of silver, resulting in an inefficient use of material. Until now, it was not clear which phenomenon is responsible for this thickness growth. In this paper, the existence of extra lattice defects in such crystals is documented and models for their effects on the thickness growth are presented.

## 2. Experimental

With a double jet method, AgNO<sub>3</sub> and NaCl are added to a mixture of gelatine, water and an adequate amount of adenine for the stabilisation of the {111} surfaces. The growth procedure is started with a nucleation phase at high supersaturation to introduce the twins necessary for the tabular growth. This is followed by a physical ripening and a long growth phase, with increasing addition rate. The crystals are produced at a temperature of 55°C in the nucleation phase and are ripened and grown at 70°C. The pH was fixed at 6.0 during the entire growth process.

For the preparation of the samples for TEM investigation, 50 µl of the emulsion is diluted in 50 ml of distilled water. A drop of this mixture is placed on a copper grid, covered with a carbon foil. The microscopes used for this investigation are a Philips CM20 and a Philips CM200 microscope. In order to avoid radiation damage during examination, the samples were cooled with liquid nitrogen in a Gatan double tilt cooling holder. The working temperature was approximately 100 K.

For the investigation with scanning electron microscopy (SEM), 100 µl of the emulsion is diluted in 50 ml of distilled water. 1 ml of this solution is filtered through a polycarbonate filter. Next, a piece of this filter is attached to a copper holder and a thin layer of gold is sputtered on top of it. The microscope used is a JEOL JSM5600 with an accelerating voltage of 30 kV. No specific precautions were needed to avoid radiation damage, since the crystals appeared to be stable enough for the investigation of their morphology.

## 3. Results

### 3.1 Tabular crystals

A typical example of a tabular crystal with its corresponding diffraction pattern is shown in figure 1. As

for silver bromide, twins with twin planes parallel to the (111) tabular face are present as can be deduced from the diffraction pattern in figure 1b. If the first variant reveals a [uvw] zone in the diffraction pattern and the twin plane has Miller indices (hkl), then the second variant produces a [u'v'w'] zone in the same diffraction pattern. The latter indices can, if necessary after multiplying with the common denominator, be calculated from <sup>5</sup>:

$$\left\{ \begin{array}{l} u' = \frac{(h^2 - k^2 - l^2)u + 2hkv + 2hlw}{h^2 + k^2 + l^2} \\ v' = \frac{(k^2 - h^2 - l^2)v + 2hku + 2klw}{h^2 + k^2 + l^2} \\ w' = \frac{(l^2 - h^2 - k^2)w + 2hlu + 2klv}{h^2 + k^2 + l^2} \end{array} \right. \quad (1)$$

The position of a u'v'w' reflection of one variant in the basis of the other variant can be determined by applying the same equations. Application of these equations to the diffraction pattern in figure 1b indicates that two variants and at least one {111} type twin plane parallel to the tabular face are present. The first variant in figure 1b is oriented along a [213] zone. The reflections with subscript 1 and their vector combinations belong to this zone. The equations above show that if the twin variants are separated by a (111) twin plane, the second variant is oriented along a [231] zone. The reflections with subscript 2 belong to this second zone. All other reflections are due to double diffraction: if the twin variants overlap the electron beam can be diffracted for a first time in the first variant and this diffracted beam can be diffracted again in the second variant. This will give rise to reflections that lie on a position that is a vector combination of a reflection of the first variant and a reflection of the second variant. This diffraction pattern proves that two twin variants and at least one twin plane parallel to the (111) tabular face are present, but it is not possible to determine the exact number of twin planes in the crystal.

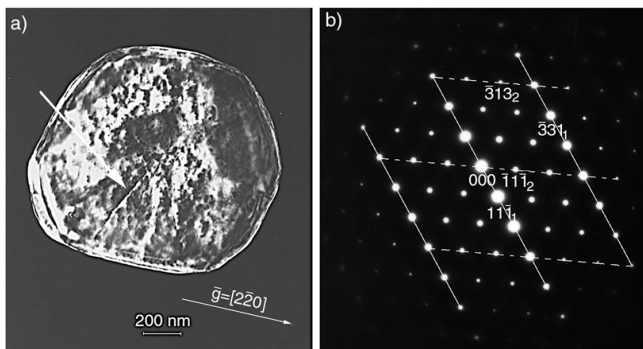


Figure 1. a) Dark field image of a tabular crystal with a dislocation (white arrow), b) a diffraction pattern obtained after rotating over 22° around a [-422] axis, indicating the presence of twin variants

A second type of defects observed in these crystals, are dislocations parallel to the top surface as indicated with a white arrow in fig.1a. From extinction conditions the Burgers vector can be determined to be parallel to a  $\langle 110 \rangle$  direction. From literature it is known that dislocations with a Burgers vector of  $a/2\langle 110 \rangle$  have the lowest energy in a silver chloride crystal and are thus most likely to occur. No direct correlation between the crystal shape and the occurrence of dislocations could be established.

The majority of the tabular crystals have a more or less hexagonal shape when seen in plan view, and a minority is triangular. However, despite the addition of the adenine, the {111} planes, on top as well as on the edges, are partly dissolved, resulting in a rounded shape and a mottled appearance.

### 3.2 Crystals with an incomplete microtwin

As indicated above, not all crystals are tabular. Depending on the growth conditions 10 to 30 % of the crystals have grown significantly in the third dimension. In all thick crystals, twins with a twin plane that is not parallel to the tabular face can be recognised. Two configurations occur more often and will be discussed in detail. Within this discussion the twins with a twin plane parallel to the (111) basal plane will be called “parallel twins”, while the twins with a twin plane that is not parallel to the (111) basal plane will be called “non-parallel twins”.

A typical example of this type of crystals is shown in figure 2. The dark field image of figure 2a shows a fringe contrast (arrow) caused by one or more planar defects.

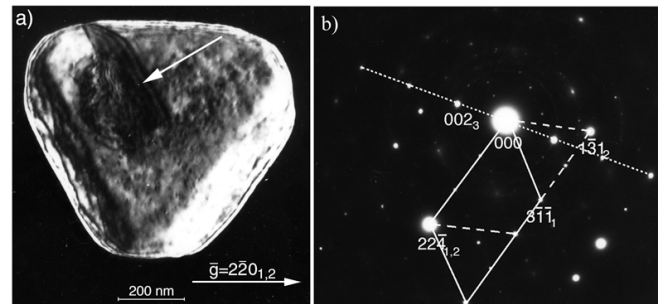


Figure 2. a) Dark field image, which shows the presence of a microtwin, indicated by the white arrow, in thick crystals of group 1. b) Diffraction pattern obtained after rotating over 11.5° along a [22-4] direction indicating the presence of 3 twin related variants

In order to determine the type of defect an analysis of different diffraction patterns was performed. The diffraction pattern in figure 2b, was obtained after rotating over 11.5° from the (111) zone around a [22-4] direction and shows that at least three different twin variants must be present. The first variant is oriented along a [354] zone and its reflections are marked with a subscript 1. As the twin plane between those two variants is parallel with the (111) plane, the second twin variant will be observed along a [534] zone, according to the formula given in the previous section. Reflections marked by a subscript 2 belong to this second variant. Both variants overlap resulting in

reflections due to double diffraction. The reflections on the dotted line in fig. 2b can be explained under the assumption of the presence of a third variant obtained by twinning on a (-111) plane. According to equation (1), this third variant will be oriented along a [710] zone. In figure 2b only the 002 reflections belonging to this zone are visible and are indicated by a subscript 3. All other reflections are diffracted too far away from the transmitted beam. This assumption complements the interpretation of all reflections of the diffraction pattern and also all other diffraction patterns, observed in this study, can be composed using these three different variants.

In order to determine the location of the third variant, an image was obtained selecting the  $002_3$  reflection. In this image the third variant corresponds with the bright area and it was established that this area corresponds with the fringe patterned area in fig. 2a. The third variant is limited by two parallel twin planes that partly overlap under the conditions of figure 2a. Because these twin planes lie very close to each other this defect is called a microtwin. The contrast induced by a microtwin consists of thickness fringes where the twin planes do not overlap, with either stacking fault fringes or no fringes in between. All fringes lie parallel to the intersection line of the twin planes with the basal plane. This is consistent with our observations, since the fringes in figure 2a are parallel to a [02-2] direction which is also the direction of the intersection line between the (-111) twin plane and the (111) basal plane.

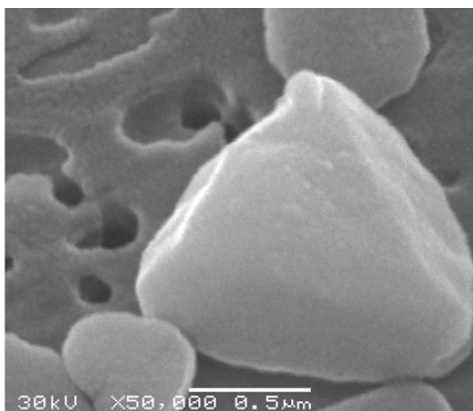


Figure 3. SEM image of a thick crystal with a microtwin, revealing the shape of a thick tabular crystal.

To determine at what time during the processing stage the microtwin is formed, samples that have been taken from the emulsion at different moments during the growth process were examined. The non-parallel twins are already observed at the end of the chemical ripening and most probably they are already formed during the nucleation phase, at the same moment or immediately after the formation of the twins that induce the tabular growth.

The shape of the projection of the crystal in figure 2 on the basal plane is still a hexagon, but in most cases three long and three shorter sides are formed. The thickness fringes on the side of the crystal indicate that the thickness of the top variant increases towards the centre of the crystal,

when observed in plan view. A SEM investigation confirms this suggestion as seen from figure 3. Although, it is not possible to determine whether or not this crystal contains a microtwin that ends inside the crystal, the projection of this crystal on the basal plane corresponds with the TEM-images. Also the small indent on top of the crystal could be an indication of the presence of an internal defect, possibly the microtwin. The SEM image also shows that the side surfaces enclose an acute angle with the basal plane, which is in practice an angle of  $70.5^\circ$ .

### 3.3 Bicrystals.

The morphology and defect structure of a second group of thick crystals can be deduced from a combination of the SEM and TEM images of figure 4. From the SEM-image in figure 4a the three-dimensional morphology can be deduced. The crystal consists of a thick tetrahedron shaped part and a flat triangular or trapezoidal part, as also confirmed by TEM-images. Moreover, at the transition from the thin to the thick part a triangular shaped contrast was found indicated by the white arrow in figure 5b. Moreover, it is possible to select a beam that has been diffracted only by the region of the triangular contrast. This indicates that again a third twin variant is present and that the contrast is due to a twin.

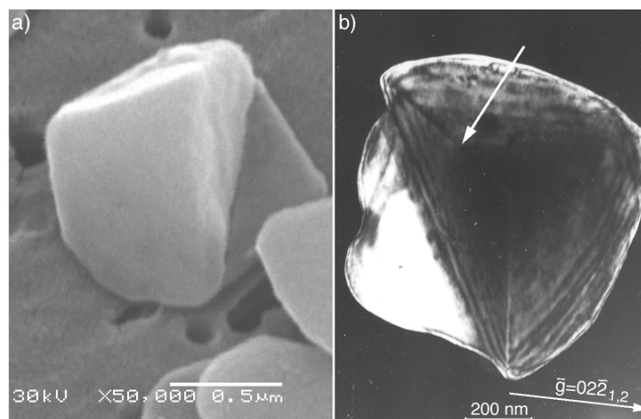


Figure 4. a) SEM image and b) Dark field TEM image of a thick crystal of group 2 using a reflection common to the first and second variant. A triangular fringe contrast due to a non-parallel twin plane, indicated by the white arrow is visible

The diffraction pattern in figure 5a confirms that a non-parallel (1-11) twin is present. A first variant is oriented along a [234] zone. The reflections belonging to this zone are marked with a subscript 1. The second variant is oriented along a [432] zone. Applying equation (1) it can be determined that the twin plane is a (111) plane. The reflections of this zone are indicated with a subscript 2. Both zones are thus mirrored with respect to the axis perpendicular to the 2-42 reflection. Both variants overlap, giving rise to double diffraction. Also a third variant occurs which is oriented along a [052] zone. Applying equation (1) indicates that the twin plane limiting the first and third variant is a (1-11) plane. Only the 200 direction with reflections marked by a subscript 3 is visible in the

diffraction pattern. Also this variant overlaps with the other two variants giving rise to double diffraction. All reflections in the diffraction pattern are now explained for and no indications were found that other twins are present. The angle between the two twin planes is again the angle between two  $\langle 111 \rangle$  planes. From the SEM image in figure 4a combined with the location of the TEM-contrast in 4b, it can be determined that the angle is acute and thus  $70.5^\circ$ .

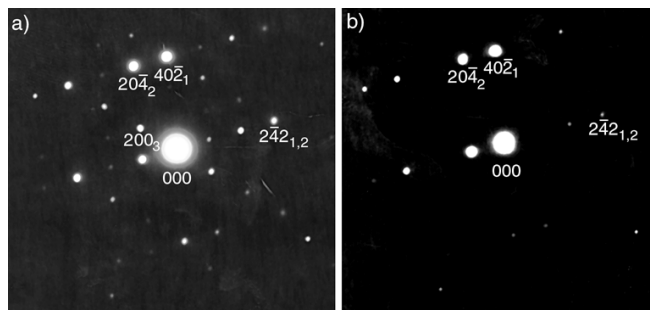


Figure 5. a) Diffraction pattern showing the presence of three twin variants. b) Corresponding diffraction pattern of the flat part that contains only two twin-variants.

The TEM images of the flat part show no contrast indicating the presence of extra defects. This means that only planar defects parallel to the basal plane can be present. From the analysis of the diffraction patterns the presence of only two twin variants in the flat part can be deduced. The diffraction pattern of figure 5a was obtained from the entire crystal and shows reflections belonging to the three variants. For the diffraction pattern in figure 5b, an area was selected within the flat part. As expected, the reflections of the third variant have entirely disappeared since this variant falls outside the selection. All other reflections, however, are still present, which proves that the tabular twins are also present in the flat part.

The shape of the flat part of the crystals, projected on the (111) basal plane, varies from a triangle to a trapezoid. Due to the dissolution of the crystal, the edges of the flat part are often rounded, troubling the determination of their direction, as in fig. 4b. Occasionally, a well-configured bicrystal is observed. For those, a typical half hexagon is formed always limited by  $[110]$  traces. This also indicates that the edge planes of the flat part of the crystal are  $\{111\}$  or  $\{100\}$  planes, like for the tetragonal part.

## 4. Discussion

### 4.1 Tabular crystals

As in AgBr, the anisotropic growth of AgCl  $\{111\}$  tabular crystals is induced by the presence of the parallel twins. Although more dislocations were observed in AgCl than in AgBr  $\{111\}$  tabular crystals, no evidence for any influence on the growth process could be found. Indeed, dislocations can in principle cause accelerated growth in one direction, as was shown for AgCl  $\{100\}$  tabular crystals<sup>6</sup>. However, many examples, e.g. the crystal in figure 1a, show that no accelerated growth of the edge at which a dislocation ends,

has occurred. Moreover, Li et al.<sup>7</sup> have calculated the speed of growth of a side face where a twin plane or a dislocation emerges, for different values of supersaturation. They conclude that the speed of growth at the emergence of a twin plane is higher than at the emergence of a dislocation, except for very low values of supersaturation, which do not occur here. This confirms that in tabular  $\{111\}$  AgCl crystals the shape of the crystals is determined by the presence of twin planes and not by the dislocations.

### 4.2 Thick crystals

In this section, the influence of the non-parallel twins on the morphology of the crystals will be discussed. Goessens et al.<sup>8,9</sup> have developed a model, based on the formation of a ridge-trough structure, to explain the presence of needles and tetrahedrons in a population of AgBr (111) tabular crystals. In both cases, non-parallel twins appeared to be responsible, with the angle between the twin planes determining the shape of the crystals. Parallel twin planes result in tabular crystals, an angle of  $70.5^\circ$  in tetrahedron shaped crystals and an angle of  $109.5^\circ$  in needles.

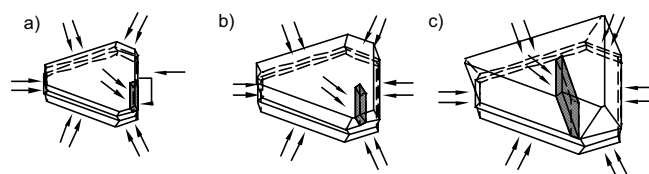


Figure 6. a-c) Successive steps in the growth of thick tabular crystals due to a non-parallel microtwin. The black arrows indicate the side faces where accelerated growth occurs.

For the thick crystals studied here, the angle between the twin planes is always  $70.5^\circ$  and therefore the growth model of the tetrahedrons has been adapted to explain the growth sequence. Figure 6 is a schematic representation of the proposed growth model. From the present observations it is not possible to determine if  $\{100\}$  as well as  $\{111\}$  faces are present. This issue will not be discussed here because on a qualitative level, the same conclusions can be drawn when accelerated growth is due to the presence of small  $\{100\}$  faces or to the occurrence of troughs formed at the intersection of the twin planes with the side faces. Furthermore, the model in fig. 6 is based on the assumption of two parallel tabular twin planes, because of the projected hexagonal shape of the crystals in the TEM-images.

Since the non-parallel microtwin has been observed in crystals after the physical ripening, it is concluded that all twins are introduced in the early stages of the growth process, i.e. when the crystals are produced under high supersaturation. First the parallel twins are introduced in such a way that three fast growing and three slower growing sides are formed. On one of the large and thus slow growing faces an accidental twin is formed that ends halfway the side face, forming an incoherent boundary (fig. 6a). After a few layers the twinned variant is overgrown by the correctly stacked variant resulting in an internal microtwin (fig 6b). The microtwin induces accelerated growth of the top

surface through the appearance of a small {100} face or a trough at this location (figs. 6b and 6c). The speed of growth of the microtwin must be comparable with the speed of growth of the side surfaces. If the speed would be much higher then tetrahedron shaped crystals would have been formed. On the other hand, if the speed would be much lower then almost no thickness growth would have occurred.

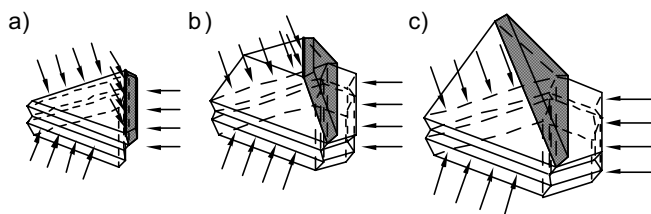


Figure 7 a-c). Successive steps in the growth of the bicrystals. The black arrows indicate the surfaces where accelerated growth occurs.

A schematic representation of the growth model of the bicrystals is shown in figure 7. It starts from a nucleus with three parallel twin planes. The number of parallel twin planes could not be determined directly from our observations, but many indications have been found which confirm our proposition. Most tabular crystals with a triangular top surface contain an odd number of twin planes. If only one parallel twin plane would be present instead of three, the growth model proposed by Goessens et al.<sup>9</sup> applies and tetrahedral crystals would be formed. Moreover, in figure 5 it was shown that the flat part contains two twin variants and thus at least one twin plane parallel to the basal plane. Since growth of the top variant is stopped after the formation of the non-parallel twin, the thick part of the crystal must contain at least two, probably three twin planes. On one of the slow growing side faces one non-parallel twin is formed (fig. 7a). In these crystals, accelerated growth occurs in three dimensions (fig. 7b and 7c). The non-parallel twin creates a small {100} face or a trough on the top surface, leading to the accelerated growth that induces the tetrahedral part of the crystal. On the other hand accelerated growth occurs along the side faces. The growth of the side faces without the non-parallel twin only enlarges the size of the tetrahedral part. The growth of the third side face induces the formation of the flat part.

The triangular to trapezoidal morphology of the flat part can be explained. While the tetrahedral part is believed to contain three parallel twin planes, and thus three fast and three slower growing edges, the flat part contains only two parallel twin planes. Consequently, all edge planes grow at approximately the same speed. Therefore the edge planes that had disappeared in the tetrahedral part, will persist in the flat part, yielding the trapezoidal shape. Small differences in growth speed and the partial dissolution of the crystal account for the shapes of fig. 5.

A minority of the thick crystals does not belong to either of these two groups. In these crystals more complex twin configurations have been observed which give rise to various, less characteristic morphologies. These crystals

have not been analysed in detail, but it is reasonable to assume that also in these crystals the twins are responsible for the specific morphology.

## 5. Conclusions

In this study it is shown that the anisotropic growth of AgCl tabular crystals with {111} surfaces is caused by the formation of parallel twins, as for AgBr. A large number of dislocations are also formed, but they do not seem to influence the morphology of the crystals. The thickness growth in 10 to 30 % of the crystals is due to the presence of twins that are not parallel to the tabular plane. Two morphologies occur more often. A first morphology is related to a defect configuration consisting of parallel twins and a non-parallel microtwin that stops inside the crystal. Arguments have been given about how this defect introduces the thickness growth and why the microtwin stops inside the crystal. A second morphology corresponds to bicrystals consisting of a tetrahedral shaped part and a flat triangular or trapezoidal part. Also in these crystals parallel twins are present and a second non-parallel twin exists that induces the thickness growth. The tabular part of the crystal is formed by the continuation of growth along the tabular twin plane edges. A minority of the thick crystals does not belong to either of these two groups. They have different defect configurations, but always contain several non-parallel twins.

## Acknowledgements

The authors would like to thank J. Van De Cruys for the SEM measurements. This work is performed with the financial support of the Flemish Institute for the Encouragement of the Scientific and Technological Research in the Industry (IWT).

## References

1. C. R. Berry and D. C. Skillman, *Photogr. Sci. Eng.*, **6**, 159 (1962)
2. J. F. Hamilton and L. E. Brady, *J. Appl. Phys.*, **35**, 414 (1964)
3. F. H. Claes, J. Libeer and W. Vanassche, *J. Photogr. Sci.*, **21**, 39 (1973)
4. K. Endo and M. Okaji, *J. Photogr. Sci.*, **36**, 182 (1988)
5. P. B. Hirsch, A. Howie, R. B. Nicholson, D. W. Pashley and M. J. Whelan, *Electron Microscopy of Thin Crystals*, Butterworths, Washington, 1965, pg.141
6. W. Van Renterghem, C. Goessens, D. Schryvers, J. Van Landuyt, P. Verrept, D. Bollen, C. Van Roost and R. De Keyzer, *J. Cryst. Growth*, **187**, 410 (1998)
7. H. Li, X.-D. Peng and N.-B. Ming, *J. Cryst. Growth*, **139**, 129 (1994)
8. C. Goessens, D. Schryvers, J. Van Landuyt, A. Millan and R. De Keyzer, *J. Cryst. Growth*, **151**, 335 (1995)
9. C. Goessens, D. Schryvers, J. Van Landuyt and R. De Keyzer, *J. Cryst. Growth*, **172**, 426 (1997)

### **Biography**

Wouter Van Renterghem is a PhD student at the EMAT laboratory of the university of Antwerp. He has studied physics at the same university from which he graduated in 1996. The subject of his research is the characterisation of

silver halide microcrystals with transmission electron microscopy. This work is in collaboration with Agfa-Gevaert, Mortsel and is financially supported by the Flemish institute for the encouragement of the scientific and technological research in the industry (IWT).